Supplementary Material

Synchronously improved graphitization and surface area in 3D porous carbon network as high capacity anode material for lithium/sodium-ion batteries

Haimi Liu[a,b], Weihao Zeng[a], Yue Yang[a], Junxin Chen[a], Yuwei Zhao[a], Shichun Mu*[a,b]

[a]State Key Laboratory of Advanced Technology for Materials Synthesis and Processing, Wuhan University of Technology, Wuhan 430070, P. R. China.

[b]Foshan Xianhu Laboratory of the Advanced Energy Science and Technology Guangdong Laboratory, Xianhu hydrogen Valley, Foshan 528200, China.

* Corresponding author E-mail: msc@whut.edu.cn

Synthesis of porous-NPC:

PANi aerogel was prepared in the presence of phytic acid by oxidative polymerization according to a published procedure. Typically, 5 mL phytic acid (70%, Aladdin) was added into 15 mL deionized water, followed by the addition of 0.6 g of SiO_2 nano-particles (100 nm) into this solution. After stirring at the room temperature for 20 minute, 5 mL of aniline (99%, Aladdin) was added into this solution. 0.9 g ammonium persulphate (APS, 99%, Aladdin) was dissolved in 10 mL deionized water under stirring at room temperature. The above two solutions were mixed together and kept stewing for 12 h at 4 °C. The resultant hydrogel was washed by plenty of deionized water for two days then freeze-dried for 24 h to produce PANi aerogel for pyrolysis. To prepare porous-NPC foam, the PANi aerogel was annealed at 950 °C for 2 h under Ar atmosphere. The obtained powder was added into moderate HF solution (30% wt, Aladdin) under stirring for 24 h to remove the SiO_2 template. The reaction product was collected by centrifugation, thoroughly washed by deionized water for several times, then freeze-dried for 24 h to obtain the final product. For comparison, SiO_2 nano-particles was removed from the phytic acid solution and without HF washing, the N, P co-doped carbon (NPC) foam was then prepared by annealing the obtained PANi aerogel at 950 °C for 2 h under Ar atmosphere.

Battery assembly and electrochemical measurements:

A slurry of the active material, Super P, and polyvinylidene fluoride (PVDF) are mixed at the weight ratio of 7:2:1. N-Methyl-2-pyrrolidone (NMP, 99.5%, Aladdin) was

introduction to adjust the viscosity of the slurry. The electrodes were then coated on a copper current collector with a spreader of 120 μm, and transferred to a vacuum oven at 70 °C for 12 h. LIBs used lithium as reference electrodes and 1 M $LiPF_6$ in a mixture of ethylene carbonate/diethyl carbonate (EC/DEC, 1:1 by volume) as the electrolyte, and Celgard13501 (Celgard) as the separator. SIBs were also fabricated at the same conditions assembling with sodium as the reference electrodes, 1 M $NaPF_6$ in a mixture of ethylene carbonate/diethyl carbonate (EC/DEC, 1:1 by volume) as the electrolyte, and glass microfiber (Whatman) as the separator. The electrochemical performance was measured on the Neware Battery Measurement System with a potential window of 0.01-3 V, the cyclic voltammetry (CV) and electrochemical impedance spectroscopy (EIS) were conducted on the CHI660E electrochemical workstation.

Materials characterization:

The morphology of the sample was characterized by scanning electron microscopy (SEM) on a HITACHI S-4800 and transmission electron microscopy (TEM) on a FEI Tacnai G2 with the accelerating voltage of 200 kV. The crystalline structure of the sample was performed on X-ray diffraction (XRD) with Cu radiation of Dmax 2500 V. X-ray photoelectron spectroscopy (XPS) scans were performed on an ESCALAB 250 photoelectron spectrometer. Raman spectra was collected on Lab RAM HR800. The Brunner-Emmet-Teller (BET) surface area of the sample was measured on Micrometritics ASAP 2020 analyzer. The thermogravimetric curve (TG) of the sample was performed by STA449F3.

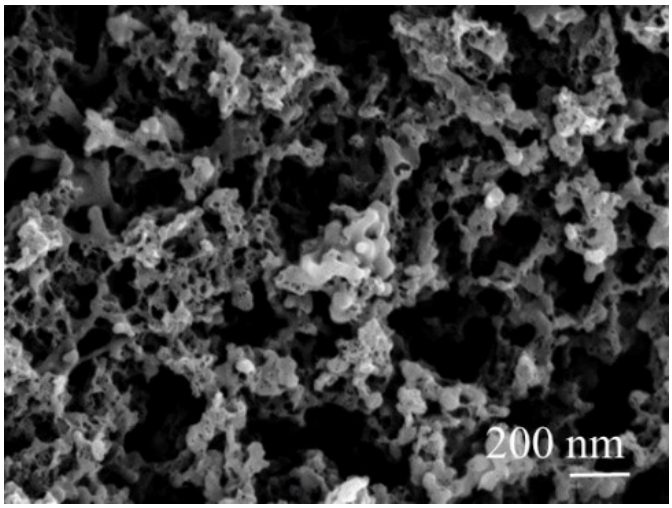

Figure S1. Low-magnification SEM image for porous-NPC.

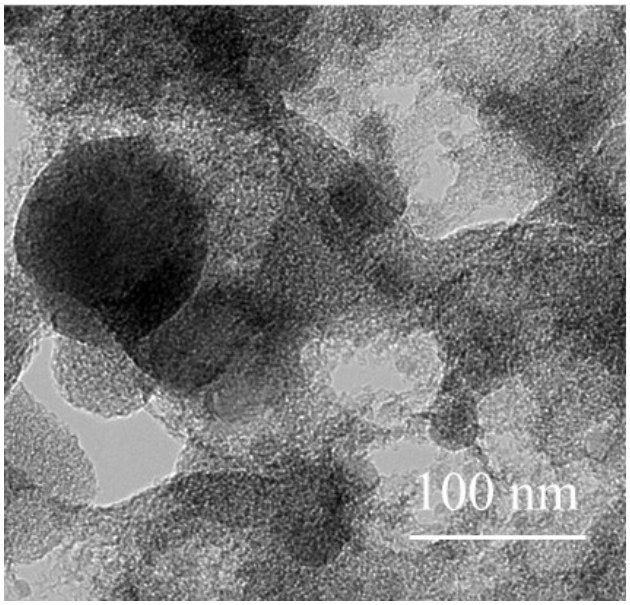

Figure S2. High-magnification TEM image for NPC

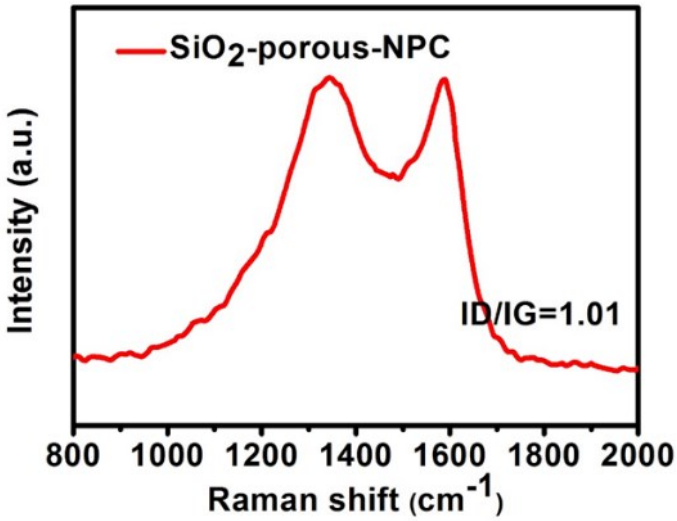

Figure S3. Raman spectra of the SiO_2-porous-NPC.

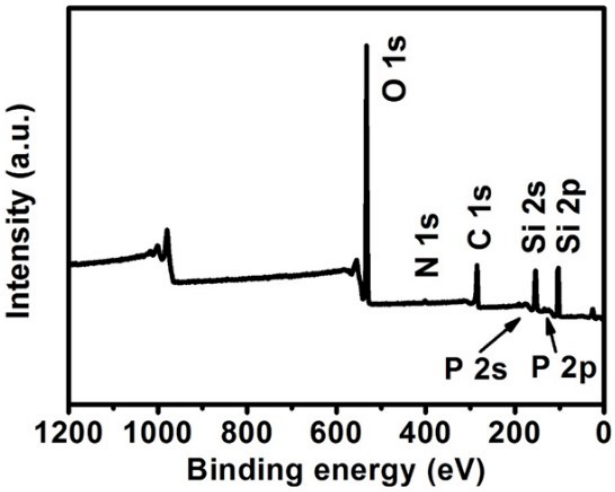

Figure S4. XPS survey spectrum of the SiO_2-porous-NPC.

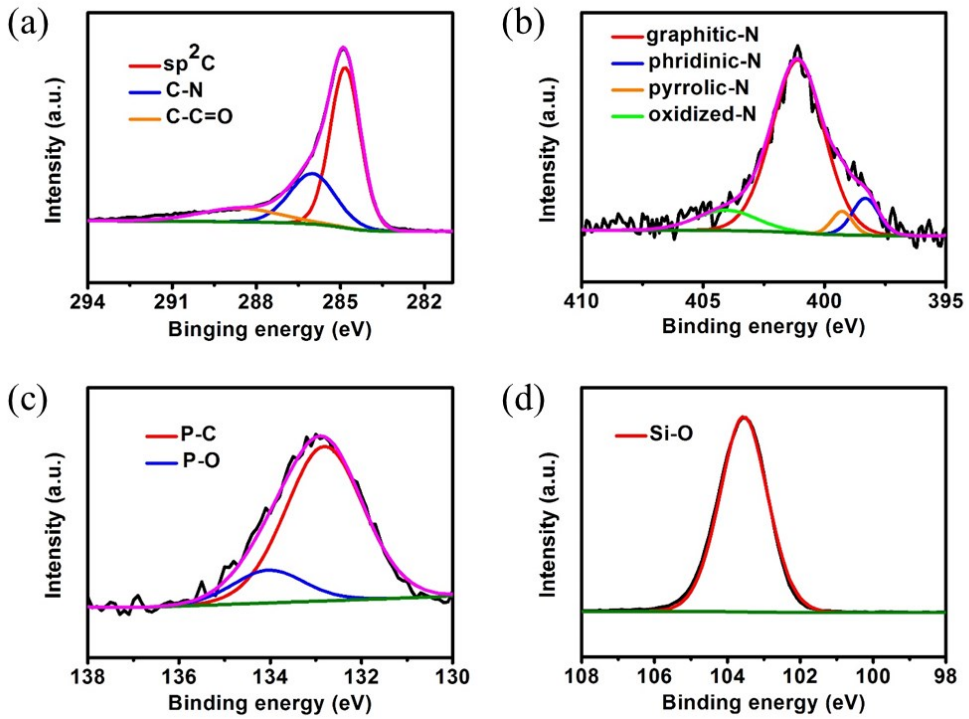

Figure S5. XPS high-resolution spectra of (a) C 1s, (b) N 1s, (c) P 2p, and (d) Si 2p of SiO_2-porous-NPC.

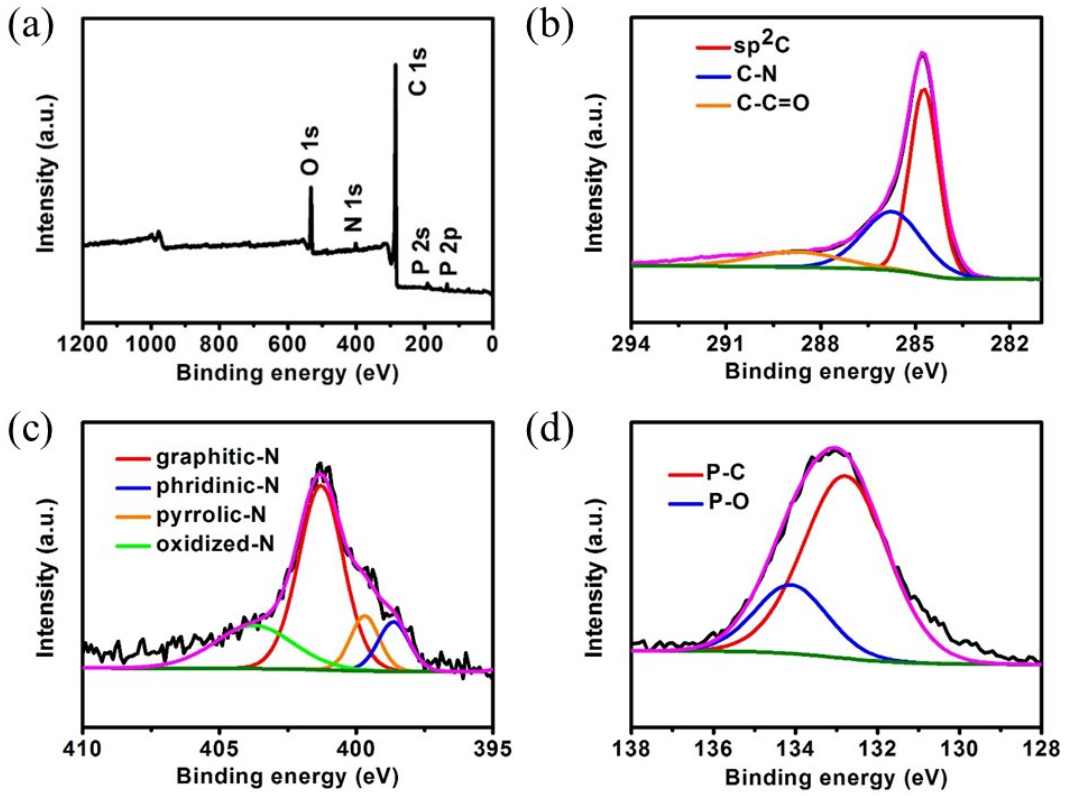

Figure S6. XPS high-resolution spectra of (a) C 1s, (b) N 1s, and (c) P 2p of NPC.

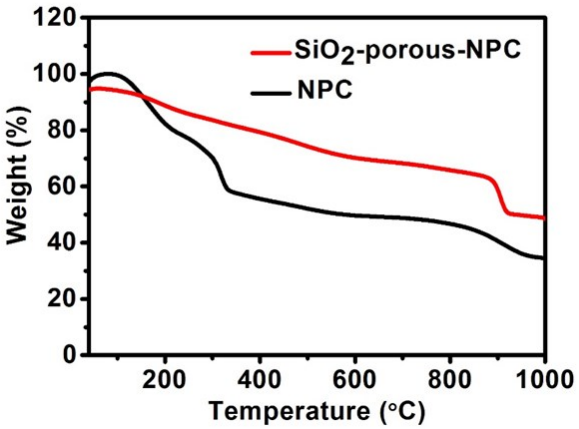

Figure S7. TG curves of the SiO_2-porous-NPC and NPC precursor.

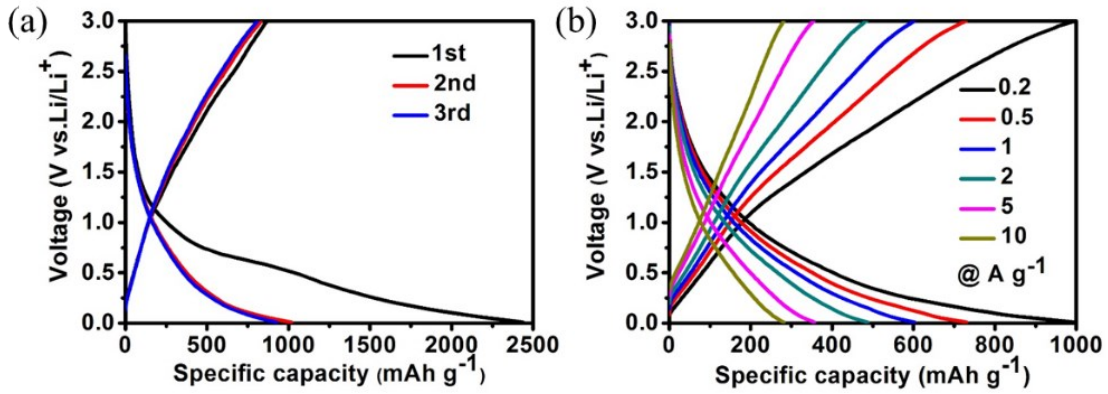

Figure S8. Electrochemical performance of the porous-NPC electrode for LIBs: (a) Charge-discharge voltage profiles at 1 A g^{-1}, and (b) Charge-discharge voltage profiles at various current densities.

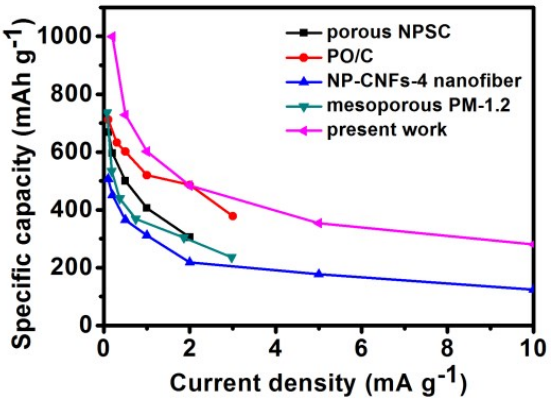

Figure S9. The comparison of electrochemical performances for the porous-NPC electrode with other reported results for LIBs.

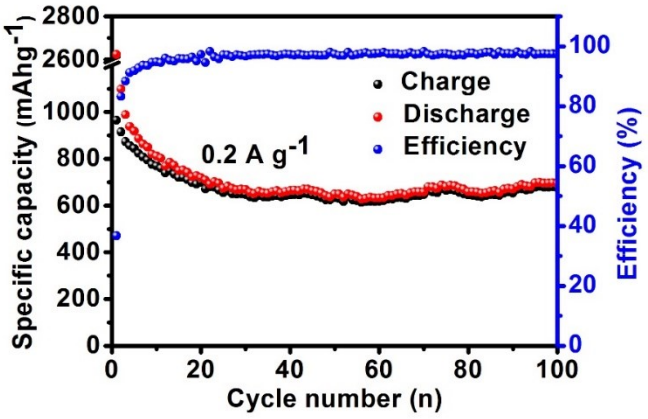

Figure S10. Long-term cycling performance of the porous-NPC electrode at a current of 0.2 A g^{-1} for LIBs.

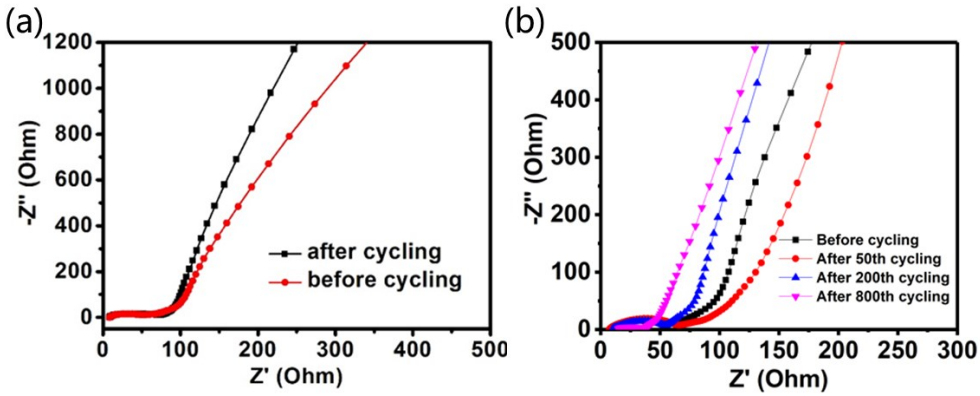

Figure S11. Nyquist plots of the porous-NPC electrode (a) before and after the cycle for LIBs, (b) after circulating different cycles for LIBs.

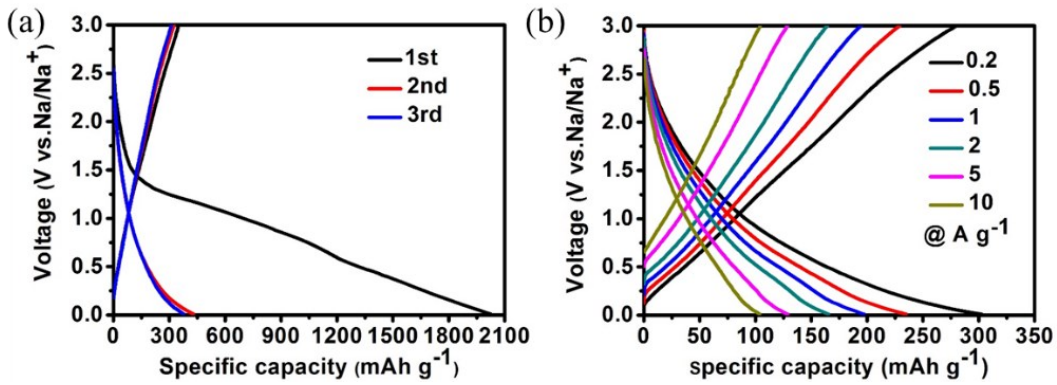

Figure S12. Electrochemical performance of the porous-NPC electrode for SIBs: (a) Charge-discharge voltage profiles at 1 A g^{-1}, and (b) Charge-discharge voltage profiles at various current densities.

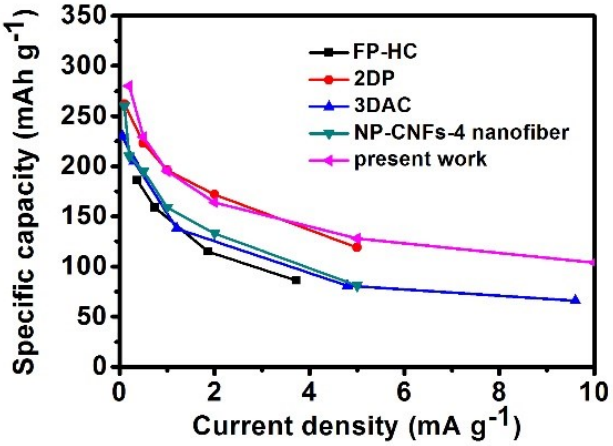

Figure S13. The comparison of electrochemical performances for the porous-NPC electrode with other reported results for SIBs.

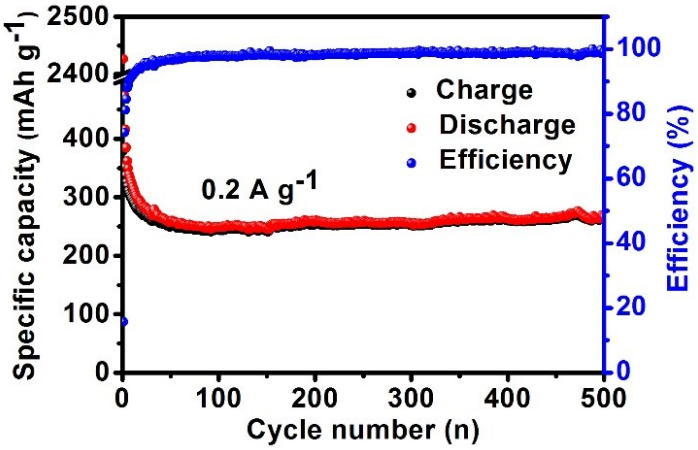

Figure S14. Long-term cycling performance of the porous-NPC electrode at a current of 0.2 A g^{-1} for SIBs.

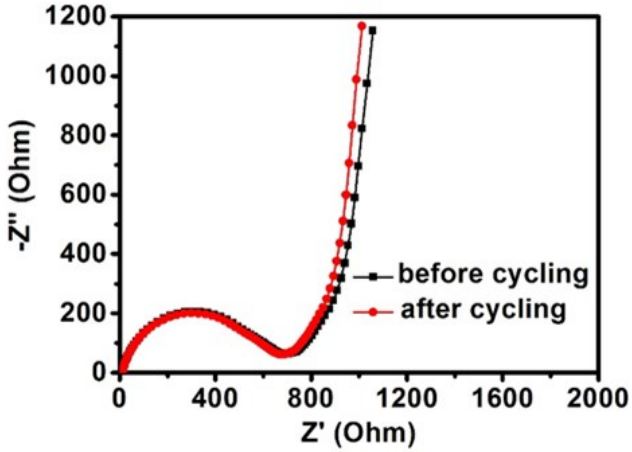

Figure S15. Nyquist plots of the porous-NPC electrode before and after the cycle for SIBs.